Heterogeneous & Homogeneous & Bio- & Nano-

CHEMCATCHEM

CATALYSIS

Accepted Article

Title: Solketal formation in a continuous flow process over hierarchical zeolites

Authors: Jolanta Kowalska-Kuś, Agnieszka Held, and Krystyna Nowińska

To be cited as: *ChemCatChem* 10.1002/cctc.201901270

Link to VoR: http://dx.doi.org/10.1002/cctc.201901270

A Journal of

ChemPubSoc Europe

WILEY-VCH

www.chemcatchem.org

10.1002/cctc.201901270

WILEY-VCH

Solketal formation in a continuous flow process over hierarchical zeolites

Jolanta Kowalska-Kuś*, Agnieszka Held and Krystyna Nowińska

Abstract: Glycerol ketalization with acetone to solketal, an oxygenate fuel additive, was demonstrated over hierarchical zeolites of ZSM5, Beta and Mordenite structure in a continuous flow system. Micro-mesoporous zeolites were prepared in two steps, by means of alkaline treatment with NaOH solution followed by the ionic exchange with NH_4NO_3 and a subsequent treatment with citric acid. The presence of mesopores in the modified catalysts was confirmed by N_2 adsorption/desorption measurements and TEM microscopy. Hierarchical zeolites showed superior catalytic performance and lifetime over 24 hours under mild conditions (atmospheric pressure, acetone to glycerol molar ratio of 3 : 1, WHSV of 3-8 h^{-1}, reaction temperature of 323 K). Glycerol conversion of about 90% and selectivity to solketal up to 98% have been obtained over micro-mesoporous catalysts within 24 h without any drop of performance and the symptoms of clogging. Among all hierarchical catalysts tested in a flow reactor, the very high activity expressed as solketal yield (88%) showed ZSM5 and Beta zeolites.

Introduction

Biofuels manufacturing performed by means of transesterification reaction of vegetable oil with methyl alcohol leads to the production not only methyl esters of fatty acids but also to coproduction of the significant amount of glycerol. The importance of biofuels is growing due to global warming and declining resources of fossil fuels.[1] Therefore, rapidly increasing production of biodiesel in recent years has brought about an overproduction of glycerol, which may be processed into many valuable products.[2] One of these attempts leads to solketal (2,2-dimethyl-1,3-dioxolane-4-methanol) formation (Scheme 1, product 1a), which is obtained as a product of glycerol ketalization reaction with acetone. Solketal indicates promising applications in fuel blending, plastics production and fine chemical industries.

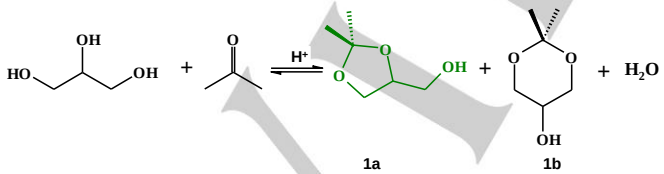

Scheme 1. Ketalization reaction of glycerol with acetone

[a] Dr J. Kowalska-Kuś, Dr A. Held, Prof. K. Nowińska,
Faculty of Chemistry
Adam Mickiewicz University in Poznań
Uniwersytetu Poznańskiego 8, 61-614 Poznań (Poland)
*E-mail: jolakow@amu.edu.pl

According to the recent studies, solketal may be used as a fuel additive to improve the octane number as well as to decrease particulates emission.[3] It is believed, that it can be an alternative to methyl tert-butyl ether (MTBE).[4] This compound can also reduce the detrimental process of the formation of insoluble solid, commonly called gum.[5]

Conventionally, the ketalization reaction is catalyzed by liquid mineral acids.[2b, 3a] However, considering the inconvenient and environmentally unaccepted liquid wastes formed as a result of separation and cleaning of the liquid catalyst, the development of highly active and easily reusable acidic solid catalysts is still a challenging problem. Numerous solid acid catalysts such as ion exchange resins (Amberlyst)[6], acidic polymers (Nafion)[5a, 7], heteropoly acids[8], as well as sulfonic acid modified mesoporous silica[9] have been tested for glycerol acetalization. Also sponge-like mesoporous silica (TUD) modified with transition metals (Zr, Hf, Sn) incorporated in the silica framework showed high activity in glycerol acetalization.[10] Recently, the functionalized mesoporous polymers (MP) appeared a new attractive group of catalysts for glycerol acetalization.[11]

Usually, the reaction of glycerol with acetone was carried out in a batch reactor, which suffers from poor mass transfer and regression of the process due to the formation of water as a by-product. These problems can be avoided by the using of a continuous flow process for the production of solketal. Till now, several research attempts have been undertaken in order to apply that method for the production of value-added chemicals and fuels from glycerol. Nanda et al.[12] and also Shirani et al.[13] performed a continuous-flow process of glycerol ketalization over Amberlyst, zeolite Beta, montmorylonite, and also Purolite® PD206. They achieved the best results using the high pressure (of about 40 atm and 120 atm, respectively). Oliveira et al.[14] using the continuous procedure for glycerol ketalization in the presence of the Amberlyst-15, K-10, and Montmorillonite catalysts carried out the process under atmospheric pressure and with acetone to glycerol ratio equal to 20 with high glycerol conversion. Even though, Amberlyst shows very high activity and relatively high stability (up to 24 h), the necessity of the catalyst regeneration performed with diluted sulfuric acid, resulting in the formation of troublesome waste, constitute a significant limitation.

Considering the above, zeolites could be considered as attractive catalysts in the synthesis of solketal. The wide range of applications of zeolites in the petrochemical industry[15] results from their strong acidity, high thermal stability, easy regeneration and a relatively low price. However, the use of zeolites of different structures (ZSM5, Beta, Mordenite, and HY) in glycerol ketalization in a batch reactor[16] ended with a moderate success. Only hydrophobic Beta zeolite showed relatively high glycerol conversion, while ZSM5, Mordenite, and HUSY zeolites, despite their high acidity, showed rather low glycerol conversion, which was attributed to their hydrophilic nature [16, 17] and also in case of ZSM5 zeolite to microporosity, resulting in diffusion

limitation.[16, 18] The above problem can be overcome by the use of hierarchical micro-mesoporous zeolites. Recently, a number of papers describing the synthesis of hierarchical zeolites of various structures, as well as their potential application have been published.[19] Hierarchical zeolites of ZSM5 structure have been successfully applied for a number of different processes such as Methanol-to-Aromatics (MTA) process,[20] glycerol etherification,[21] and dehydration,[22] and also for benzene to phenol oxidation.[23] Desilicated Mordenite and Beta zeolites also showed benefits of generated mesoporosity in various catalytic processes.[24]

In this work we applied a continuous flow system operating under atmospheric pressure for solketal synthesis with the successful usage of hierarchical zeolites of ZSM5, Beta, and Mordenite structure. These results offer milder reaction conditions, compared to these presented in the literature. The continuous flow process is significantly more favourable and more efficient than the batch system, particularly considering the industrial application. The use of atmospheric pressure simplifies the process and makes it cheaper, even though a small amounts of solvent has to be separated. The possible application of micro-mesoporous zeolites as catalysts in continuous flow system seems very attractive taking into account the easy commercial availability of the initial material and its relatively effortless modification. Additionally, the relatively short contact of product comprising water with catalysts in continuous flow process limits both solketal hydrolysis and also the formation of thermodynamically more stable isomer (six-membered ring ketal) resulting in almost 100 % selectivity of desirable product.

Results and Discussion

Catalysts characterization

The applied zeolite catalysts were characterized comprehensively for their textural and chemical properties.

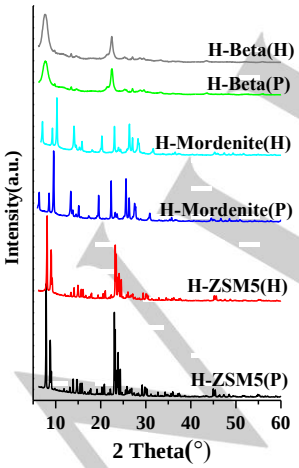

Figure 1. 1 XRD patterns of parent and hierarchical zeolites.

On the base of XRD patterns it has been indicated that all hierarchical catalysts of ZSM5, Beta, and Mordenite structure, obtained by desilication procedure and the subsequent treatment with citric acid, preserved the initial zeolite structure with somewhat lower crystallinity (Fig. 1, Table 1). No additional phase was recognized in the XRD patterns of these hierarchical catalysts. The highest decrease in the crystallinity was observed for modified H-Mordenite(H) catalyst (70% of the initial value). Lowering in the crystallinity of hierarchical Mordenite may result not only from the desilication process but also from the partial dealumination of Mordenite structure, which is confirmed by the increase in Si/Al ratio (Table 1). A similar decrease in crystallinity for Mordenite with Si/Al ratio of about 20 as a result of acidic treatment was reported by Ban et al..[25]

The modification of zeolites by desilication with following acidic treatment results in a change in their textural properties (Table 1). Particularly an increase in the surface area and a considerable growth of total porosity have been observed.

These changes are the most conspicuous for the H-ZSM5(H) sample. The applied modification procedure brings about the changes in the pore structure of ZSM5 zeolite, which is presented by low temperature N_2 adsorption-desorption measurements (Fig 2A). According to IUPAC classification, isotherm of the parent ZSM5 catalyst can be assigned as a type I, what is in accordance with their microporous nature. In turn, the hierarchical catalyst obtained by the applied procedure was characterized with the isotherm of type IV indicating the mesopores formation (Fig 2A).

The precise analysis of N_2 adsorption/desorption isotherms of modified ZSM5 (Fig. 2A) indicates the hysteresis loop at p/p_0 in the range of 0.4-0.8 and poorly pronounced hysteresis loop at about 0.9.

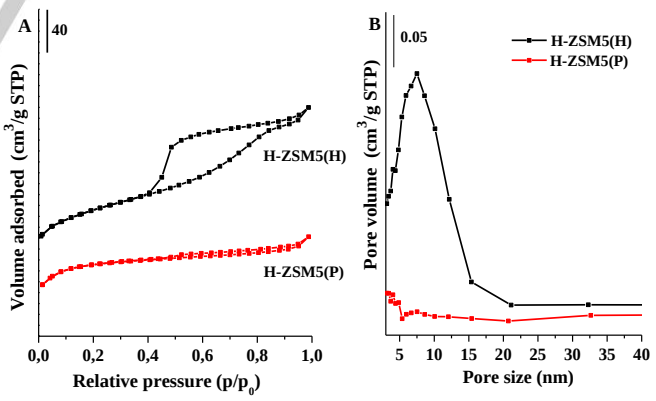

Figure 2. (A) N_2 adsorption/desorption isotherms and (B) BJH pore size distribution derived from the adsorption branch of the isotherm of parent and hierarchical H-ZSM5 zeolites.

Table 1. Crystallinity, textural properties and the number of acid sites (from TPD of ammonia) of parent and hierarchical zeolites.

Zeolite	Si/Al molar ratio[a]	S_{BET}[b] (m^2/g)	Sext[c] (m^2/g)	Vmeso[d] (cm^3/g)	Vmicro[e] (cm^3/g)	Relative Crystallinity[f]	Low NH_3 des. (μmol/g)	High NH_3 des. (μmol/g)	Total NH_3 des. (μmol/g)
H-ZSM5(P)	28.0	187	54	0.04	0.16	100	294	172	466
H-ZSM5(H)	22.1	340	215	0.33	0.10	81	530	350	880
H-Beta(P)	12.0	490	159	0.50	0.21	100	570	431	1001
H-Beta(H)	12.0	539	259	1.02	0.19	95	546	265	811
H-Mordenite (P)	17	398	74	0.14	0.21	100	416	258	674
H-Mordenite(H)	20.2	410	129	0.45	0.18	70	413	349	762

[a]Molar ratio determined by F-AAS, [b]BET specific surface area, [c]external surface, [d]mesopore volume, [e] micropore volume, [f]Crystallinity calculated from XRD patterns

According to the literature data[26] the hysteresis loop in the partial pressure region (p/p_0 0.35-0.6) is associated with framework porosity, while the hysteresis loop at high partial pressure (p/p_0>0.8) shows the textural meso- and/or macroporosity. On the other hand, the sharp increase in nitrogen uptake at p/p_0>0.9 is indicative of some amount of interparticle mesoporosity.[26a] Taking into account the above data one may suggest the formation of both the framework porosity as well as also intercrystalline porosity in modified ZSM5 sample. It is in accordance with SEM and TEM images indicating the clear corrosion of ZSM5 particles (Fig. 3) and also the presence of interparticle space (Fig. 4) as a result of modification process.

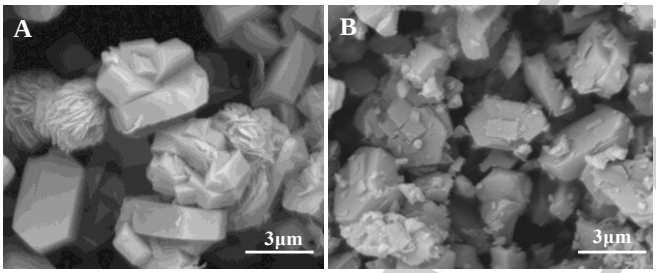

Figure 3. SEM images of parent (A) H-ZSM5(P) and hierarchical (B) H-ZSM5(H) zeolites.

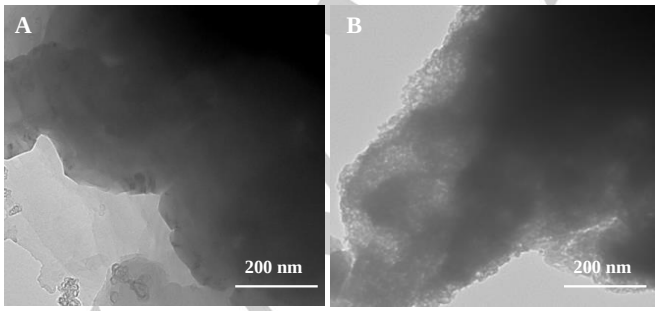

Figure 4. TEM images of parent (A) H-ZSM5(P) and hierarchical (B) H-ZSM5(H) zeolites.

The increase in the total pore volume for modified H-ZSM5(H) zeolite at the reduced volume of micropores noted in the initial sample (Table 1) indicates a formation of framework porosity during the modification procedure (Fig. 2B). The pore distribution calculated according to BJH method from the adsorption branch of the isotherm[27] for modified ZSM5 zeolite, presented in Fig. 2B, displays a broad peak centered with maximum diameter of about 8 nm, pointed to a significant amount of mesopores formed by desilication process with following acidic treatment.
In contrast to ZSM5, belonging to medium pores zeolites,[28] parent Mordenite and Beta zeolite are attributed to group of large pores zeolites. Mordenite contains one dimensional 12R channel system and also 8-membered side narrow channels,[29] while Beta zeolite comprises mainly 12R large pores.[28]

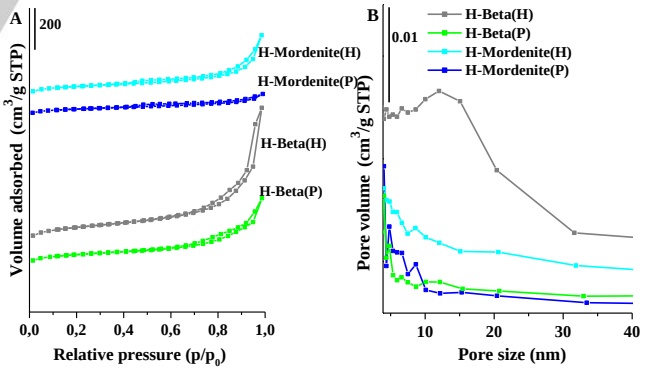

Figure 5. (A) N_2 adsorption/desorption isotherms and (B) BJH pore size distribution derived from the adsorption branch of the isotherm of parent and hierarchical H-Mordenite and H-Beta zeolites.

Isotherms of the parent zeolites of Beta and Mordenite structure show small hysteresis loops indicating some mesoporosity (Fig 5A). Adsorption of N_2 at p/p_0>0.8 and p/p_0>0.9 for these two samples was attributed to the filling of the mesopores, originated from the texture and the presence of interparticle

voids in Beta and Mordenite materials, respectively. Desilication process with the following treatment with citric acid results in the increase in the hysteresis loops at (p/p_o>0.9) indicating the formation of intercrystalline mesopores, similarly as it was suggested in the literature.[26a] The similar observation has been made by Ogura et al.[30] and also Tao et al.,[31] who indicated the formation of interparticle pores as a result of alkaline treatment. These intercrystalline pores facilitate access of reagents to active centers which were restricted in the parent samples.

Analysis of the pore size distribution in parent Beta zeolite indicates the predominance of pores of about 5 nm and a small amount of pores at ca. 11 nm, suggesting the existence of inhomogeneous pores. In turn, H-Mordenite(P) sample is characterized mainly by the pores with maximum around 4 nm and some amount of mesopores with broad maximum at about 15 nm. Compared to parent samples, the pore size distribution of modified H-Beta(H) and H-Mordenite(H) zeolites indicates clear enlargement of mesopores with maxima in the range of 15 and 20 nm, respectively (Fig 5B). Interestingly, the volume of micropores remained practically unchanged. The formation of mesopores in hierarchical Beta and Mordenite zeolites was accompanied mainly by the increase in external surface area. Such behavior can be explained by the formation of external mesopores not at the expense of micropores. The formation of external porosity may also be confirmed by SEM images recorded for parent and modified Beta and Mordenite zeolites. Even though, the SEM images of parent and modified samples differed slightly, some diminution of crystallites and surface corrosion of modified ones was noted (Fig. 6). Considering the significant increase in the external surface, relatively high p/p_0 related to hysteresis loop and SEM images it seems that newly created mesopores in the modified Beta and Mordenite zeolites have mainly interparticle nature.

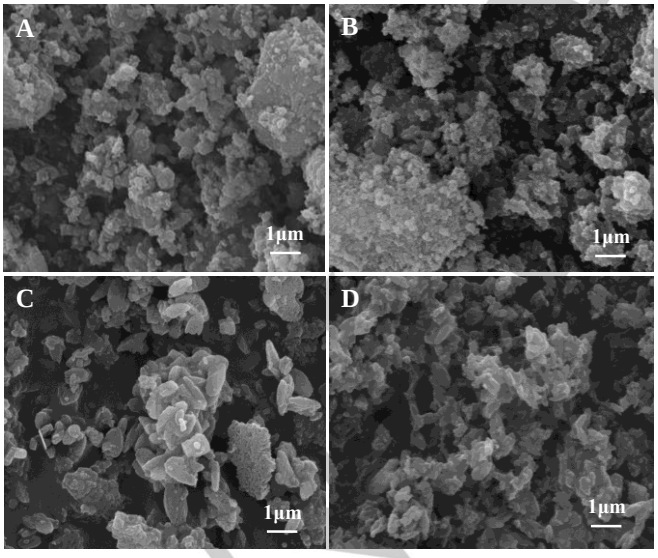

Figure 6. SEM images of parent and hierarchical zeolites (A) H-Beta(P), (B) H-Beta(H), (C) H-Mordenite(P), and (D) H-Mordenite(H).

Two-step method of the modification of parent zeolites differently affects the Si/Al ratio of the studied samples. Desilication of Beta zeolite with the following acid treatment does not change its Si/Al ratio. However, the lowering of its crystallinity as well as an increase in the mesopores volume indicate both silica removal and aluminum extraction from Beta structure as a result of performed procedure.

Otherwise, modification of Mordenite results in the increase in Si/Al ratio. It is in accordance with Li et al.[32] and Stefanidis et al.[33] observations. The quoted authors have shown that desilication of Mordenite with following acidic treatment results in Si/Al increase as a consequence of the partial dealumination.

The desilication procedure with the following acidic treatment results in the change of Si/Al ratio also of ZSM5 zeolite (Table 1). The data estimated by F-AAS analysis indicate that the Si/Al ratio of hierarchical ZSM5 zeolite was lower than that of the microporous catalyst. It suggests, that silicon corrosion took place to a larger extent followed by the aluminum debris removal, formed as an effect of the initial desilication process.[34]

The applied modification of zeolite structures brought about alteration in surface nature of the modified materials. The influence of the used procedure on the nature of surface acidity was estimated on the base of FTIR spectra recorded in the range of OH groups and also from TPD of ammonia.

FTIR spectra in the range of OH groups are presented for parent, desilicated zeolites (after the first step of the procedure), and for the samples with the following treatment with citric acid (the second step of the modification). The analysis of the FTIR spectra after each step of the applied modification allows for an in-depth understanding of the changes in the acidity of the studied samples.

FTIR spectra of parent ZSM5 zeolite in the range of hydroxyl groups (Fig. 7A) indicate the presence of the bands at 3610 cm^{-1} and 3660 cm^{-1} characteristic for Si-O_1H-Al and Si-O_3H-Al groups related to acidic sites of different strength. A sharp band at 3745 cm^{-1} is ascribed to isolated Si-OH silanol groups located on the external surface (Si-$OH_{iso/ext}$ at 3745 cm^{-1}). Desilication procedure by alkali treatment results in a significant increase in the intensity of Si-$OH_{iso/ext}$ (3745 cm^{-1}) and appearance of weak band at about 3730 cm^{-1} attributed to the formation of framework defects, related to internal isolated OH groups (Si-$OH_{iso/int}$).[35] This confirms the extraction of Si species and the development of mesoporosity in the studied samples. Intensity of the bands attributed to acidic hydroxyl groups (3610 cm^{-1}) increases after desilication procedure, which may be explained by the formation of easily available Al-(OH)-Si groups. Additionally, a weak band at about 3670 cm^{-1} ascribed to the extraframework Al-OH groups of other character is also formed in desilicated samples.[36] The following acidic treatment preserves the bands at 3610, 3670, and 3745 cm^{-1} on the surface of modified ZSM5 zeolite, however of lower intensity.

FTIR spectrum of parent Beta zeolite is represented by the bands at 3610, 3670, and 3745 cm^{-1}. Desilication of Beta zeolite results in clear increase in the intensity of FT-IR bands attributed to silanol groups (3745 cm^{-1}) and small decrease in the intensity of acidic OH groups at 3610 cm^{-1} assigned to Si-OH-Al acidic sites (Fig. 7B). Alkali treatment does not influence the band located at 3670 cm^{-1} ascribed to OH groups connected to extraframework aluminum species (Fig. 7B).

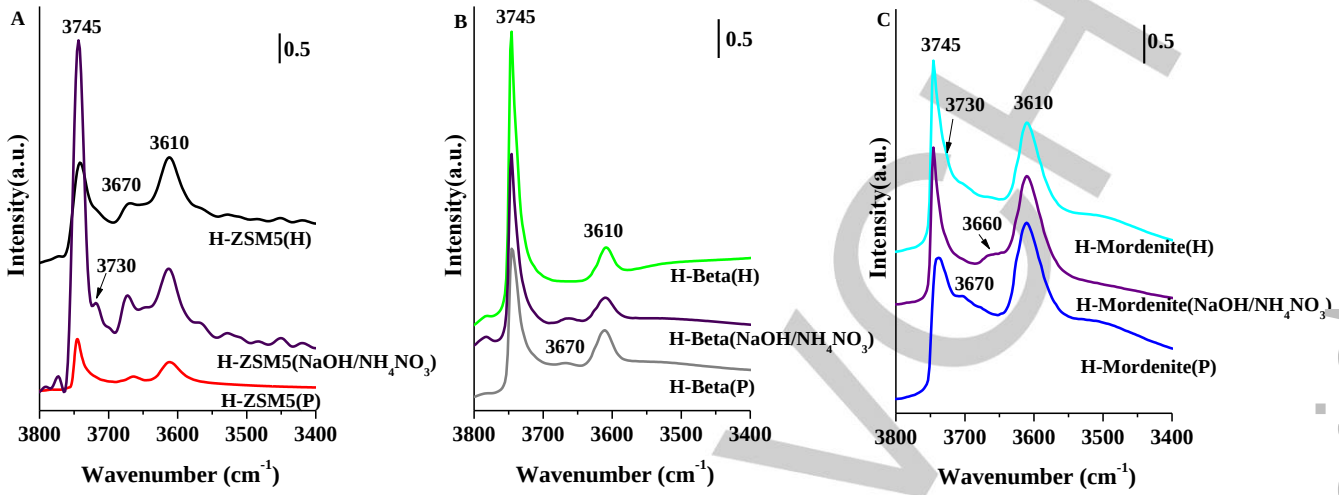

Figure 7. FT-IR spectra of hydroxyl groups recorded on parent and hierarchical zeolites: A) H-ZSM5, B) H-Beta, C) H-Mordenite.

The following treatment with citric acid results in disappearance of the band at 3670 cm^{-1}. It may be explained by relatively low stability of isolated framework aluminum in Beta structure.

When FT-IR spectra in the range of hydroxyl groups present on Mordenite (Fig. 7C) were analyzed, it has been noted that the band ascribed to Si-$OH_{iso/ext}$ groups (3745 cm^{-1}), similarly as on ZSM5 and Beta zeolites, increased in the intensity as a result of desilication process, while the band characteristic of acidic Si-O_1H-Al groups (3610 cm^{-1}) changed slightly. Additionally, the weak band characteristic for internal OH groups was still present. In the spectrum of non-treated sample, similarly like in Beta parent zeolite, the band at 3670 cm^{-1} of the extraframework Al-OH groups was also present. Desilication process and further acidic treatment remove these defects. Similar observation, as a result of desilication and following dealumination of Mordenite was reported in the literature.[37]

The number and strength of acidic sites of parent and modified zeolites of ZSM5, Beta and Mordenite structure were estimated on the base of temperature-programmed desorption of ammonia and the profiles related to desorption temperature are shown in Fig. 8. The amount of acid sites can be calculated from the desorption peak area while the acid strength can be estimated from the desorption temperature. The TPD curves of both parent and hierarchical materials indicate the presence of a low-temperature desorption peak around 523 K (related to weak acid sites) and a high-temperature desorption peak at 773 K (related to strong acid sites), respectively. The number of acid centers calculated on the base of TPD of ammonia is given in Table 1. The modification process results in some alteration in the number and strength of the acid sites.

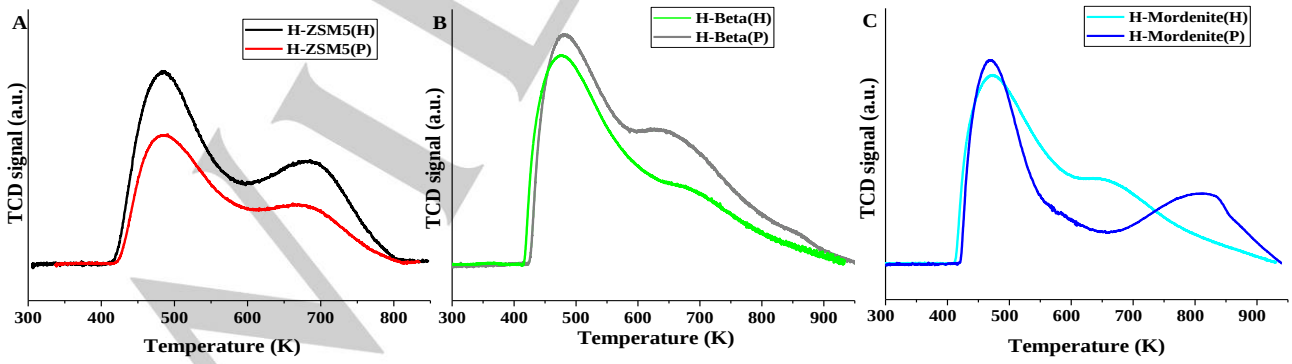

Figure 8. NH_3-TPD of parent and hierarchical zeolites: A) H-ZSM5, B) H-Beta, C) H-Mordenite.

An increase in the number of weak and strong acid centers in modified ZSM5 zeolite has been noted (Fig. 8A). According to Song et al.[38] desilication process results in the creation of more weak and strong acid sites. Increase in ZSM5 zeolite acidity is in line with some reduction of the molar ratio of Si/Al.
H-Beta(H) showed some decrease in total acidity especially in the number of strong acid sites after modification process (Fig. 8B). Vankatesha et al.[39] observed similar changes in the strength of the acid sites upon treatment with organic acids over Beta zeolite.
The applied modification practically did not affect Mordenite total acidity (Fig. 8C). However, some changes in the strength of the acid centers in H-Mordenite(H) were observed. The number of weak acid sites remains almost unchanged after modification, while the strong acidic sites (ammonia desorption of about 850 K) are transformed to the medium ones characterized with temperature of ammonia desorption of about 650 K.

Catalytic activity

Parent zeolites of different structures (ZSM5, Beta, Mordenite) as well as their hierarchical analogues were applied as catalysts for glycerol ketalization, performed in a continuous flow system at 323 K, under atmospheric pressure, with acetone : glycerol ratio equal to 3 : 1 and WHSV equal to= 3.4 h^{-1}.
Among the unmodified zeolites, both Beta and Mordenite samples showed relatively high activity for this reaction, which can be explained by the presence of 12R channels.[29] The activity of both parent zeolites decreased only slightly with time on stream. On the other hand, the microporous (parent) zeolite of ZSM5 structure showed low initial glycerol conversion (about 35 %), decreasing with time on stream up to 10 % (after 6 hours on stream) (Fig. 9).

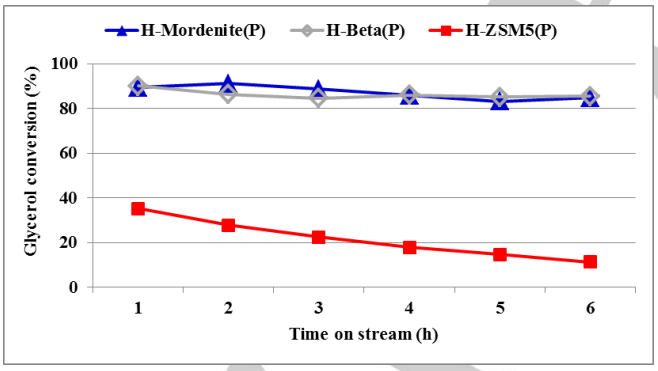

Figure 9. Glycerol conversion over parent zeolites H-ZSM5(P), H-Beta(P), and H-Mordenite(P) with time on stream.

The low activity of parent ZSM5 zeolite may be explained by diffusion limitation considering that the reagents and products show the diameter in the range of 4.3 – 5.2 Å (calculated according to the GaussView program,[40] while ZSM5 zeolite exhibits the diameter of straight channels equal to 5.3 x 5.6 Å.[28] Because of the narrow pore size the ketalization reaction on ZSM5 zeolite occurs mainly on the external surface and also at the pore entrance. Deactivation of microporous ZSM5 zeolite may be due to the blocking of micropores entrance with water formed during the reaction, especially, considering the low reaction temperature.[16b]
Modification of parent ZSM5 zeolite by means of desilication process with following acid treatment resulting in the formation of micro-mesoporous material influenced its catalytic activity in glycerol ketalization dramatically. The conversion of glycerol over hierarchical ZSM5 zeolite increased up to 90 %. (Fig. 10). Overcoming diffusion problems allowed to obtain high glycerol conversion and catalyst stability over 24 hours.

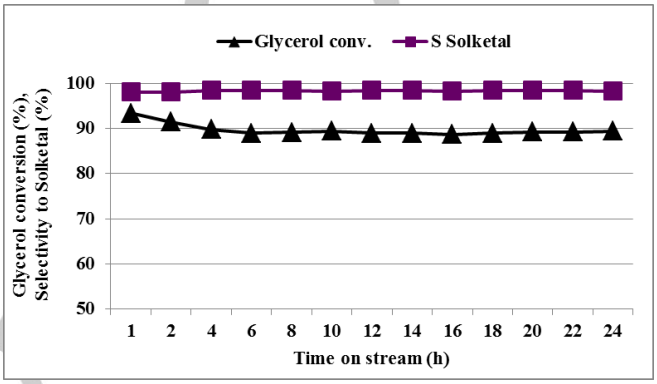

Figure 10. Glycerol conversion and selectivity to solketal over hierarchical H-ZSM5(H) zeolite with time on stream.

Hierarchization by desilication with the following acid treatment applied for modification of Beta zeolite and Mordenite caused different catalytic effect. As mentioned above, the both unmodified Beta and Mordenite zeolites, showed high activity for glycerol conversion (Fig. 9). The modification procedure did not change the glycerol conversion noticeably. The activity of unmodified Beta zeolite showed some decrease with time on stream (from 90 to 83 %), while the activity of hierarchical sample was slightly higher (Fig. S1) and remained stable (of about 90 %) for 24 hours with very high selectivity to solketal up to 98% (Fig. 11).

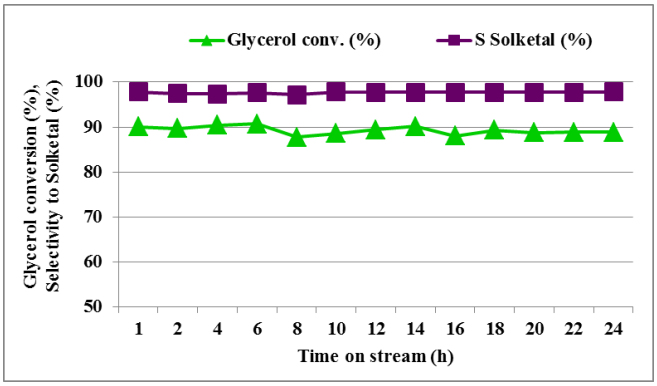

Figure 11. Glycerol conversion and selectivity to solketal over hierarchical H-Beta(H) zeolite with time on stream.

Desilication procedure with following acid treatment results in some alteration in acidity (Table 1, Fig. 8B) of modified Beta zeolite with some decrease in the number of acid sites.

Considering that, generated mesoporosity with somewhat lower amount of acidic centres, especially the stronger ones, seems to be profitable for ketalization process. Also Venkatesha et al.[39] recorded small increase in glycerol conversion over dealuminated Beta zeolite (tested in a batch reactor), when compare to unmodified one.

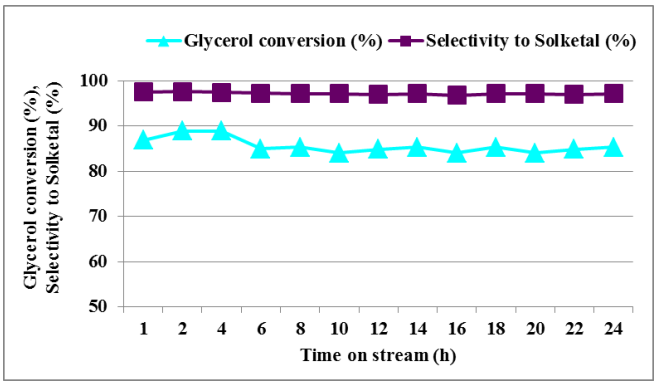

Figure 12. Glycerol conversion and selectivity to solketal over hierarchical H-Mordenite(H) zeolite with time on stream.

When hierarchical Mordenite was applied as catalyst for glycerol ketalization both glycerol conversion (of about 86 %) and also selectivity to solketal (97 %) were very similar to these recorded on parent sample (Fig. S2, 12). Some decrease in glycerol conversion (to 82 %) was noted for the both samples, parent and modified one, during the first 6 h, however, this values remained unchanged during the next 16 h (Fig. 12). The decrease in glycerol conversion noted on parent Mordenite may results from uni-demensional pore structure, which, as it was indicated in the literature, is susceptible to diffusion limitation.[25] Modified Mordenite, despite the development of mesopores (Table 1, Fig. 5B) shows also some decrease in glycerol conversion, similarly as unmodified one. According to Ban et al.[25] modification of Mordenite generates internal silanol groups (confirmed by the presence of IR band recorded at 3730 cm^{-1}) (Fig. 7C) and also silanol nests. Barbera et al.[41] indicate that the formation of internal OH groups is responsible for zeolites deactivation. According to quoted authors deactivation correlates with the ratio of internal and external OH groups expressed as I_{3730}/I_{3745}.

Analysis of Mordenite texture (Table 1) indicates the generation of mesoporosity with simultaneous decrease in the crystallinity and a slight difference in the acidity. Nevertheless, a small difference in acidity as well as some change in porosity does not influence the catalytic activity for ketalization reaction. The similar results have been reported by Tsai et al.[42] and Wang et al.[43] for the hierarchical Mordenite applied for alkylbenzene transalkylation and benzene alkylation, respectively. According to quoted authors,[44] both base and acid treated Mordenite showed the initial activity similar as for unmodified sample.

The additional experiments have been performed to estimate the effect of WHSV (Weight Hourly Space Velocity) on glycerol conversion and solketal yield and also on productivity of the main product expressed in $kg_{solketal}/kg_{cat}\cdot h$. Increase of WHSV from 3.4-8.4 h^{-1} influenced the activity of zeolites depending on zeolite structure. Increase of WHSV from 3.4 to 4.4 h^{-1} did not affect the glycerol conversion over H-Beta(H) zeolite, while the activity of H-ZSM5(H) decreased slightly.

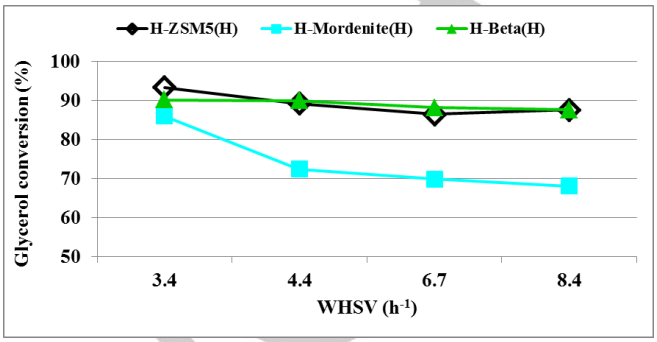

Figure 13. Glycerol conversion as a function of weight hour space velocity (WHSV) over H-ZSM5(H), H-Beta(H), and H-Mordenite(H) zeolites.

The farther WHSV growing (up to 6.7 and 8.4 h^{-1}) resulted in small decrease in glycerol conversion and solketal yield both on H-Beta(H) and H-ZSM5(H) zeolites (Fig. 13). When modified Mordenite (H-Mordenite(H)) was tested under different WHSV values, the lowering of glycerol conversion and solketal yield recorded in whole range of the applied WHSV values was more visible. It may be explained considering the influence of the modification procedure on the samples hydrophobic/hydrophilic nature, which depends on zeolite structure. According to Thommes et al.[45] modification of zeolites with the formation of hierarchical structure influences not only porosity but also Si/Al ratio, and thereby acidity, and hydrophobic/hydrophilic nature of the catalyst. Even though, the relationship of acidity and hydrophilicity index (HI) is different for different zeolite structure[46] this parameter affects acetalization process.

Hydrophobicity index calculated according to[47] changed slightly for hierarchical Beta and ZSM5 zeolites (Table S1), while this index decreased significantly for Mordenite indicating growing in hydrophilicity of the modified sample. Hydrophilic sites easily adsorb water, a by-product of acetalization reaction, which limits the access of reagents to active sites.

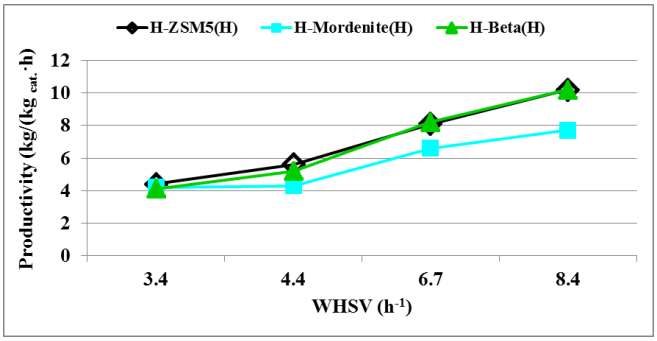

Figure 14. Solketal productivity as a function of weight hour space velocity (WHSV) over H-ZSM5(H), H-Beta(H), and H-Mordenite(H) zeolites.

The growth of WHSV value results in an increase in solketal productivity over all applied hierarchical zeolites (Fig. 14.) and simultaneously in a greater amount of water formation. Water

may be easily adsorb on hydrophilic sites thus blocking the active sites. This may be responsible for lowering in glycerol conversion with increasing WHSV value (Fig. 13), especially visible on H-Mordenite(H) (characterized with the highest hydrophilicity among the studied catalysts, Table S1).

With WHSV growing, the productivity of solketal ($kg_{solketal}/kg_{cat}\cdot h$) increases almost linearly. Considering, that with flow rate growth the clogging problems were not observed these results indicate that catalytic process operating at relatively high WHSV value (8.4 h-1) may still be modified to obtain the more economic results.

The presented results indicate that hierarchical zeolites of Beta and ZSM5 structure applied in a continuous flow system operating under atmospheric pressure show the highest productivity of solketal among the applied catalysts (2.57 [$kg_{solketal}/kg_{cat}\cdot h$]) as well as in comparison with the results presented in literature.[14]

Conclusions

Catalytic activity of hierarchical H-Beta(H) and H-ZSM5(H) zeolites demonstrates their superior performance in the reaction of glycerol with acetone ketalization carried out in a flow-system at low temperature and under atmospheric pressure. It indicates that larger pore size, created as a desilication effect in hierarchical zeolites, allows to avoid diffusion restriction of reagents and facilitates contact of the reactants with the active centers, resulting in a very high activity in the studied process. A short contact time provides the conditions for very high glycerol conversion and selectivity to solketal. The growing flow rate and increasing WHSV results in visible increase in solketal productivity. On the other hand, the generation of additional mesoporosity in Mordenite zeolite does not improve catalytic activity in glycerol acetalization, which may be due to the lowering in the crystallinity as well as its hydrophilic character, responsible for water adsorption, which limits the access of reagents to active sites.

Experimental Section

1. Materials

H-ZSM5 (Alsi Penta, SiO_2/Al_2O_3=55), H-Beta (Sigma Aldrich, SiO_2/Al_2O_3=25), and H-Mordenite (Süd Chemie, SiO_2/Al_2O_3=35) were used as parent zeolites submitted for subsequent modification. The reagents used in the experiments: glycerol (99.5 % purity), acetone (99 % purity), methanol (99.8 % purity), sodium hydroxide, and citric acid monohydrate (99.4 %) were purchased from POCH.

2. Catalysts preparation

Hierarchical micro-mesoporous ZSM5, Beta and Mordenite catalysts were prepared by means of alkaline treatment (0.2 M aqueous solution of NaOH at 353 K for 2 h) with following washing, filtration and ionic exchange with NH_4NO_3 (0.5 M aqueous solution of NH_4NO_3 at 308 K for 24 h) (desilication step) and a subsequent treatment with citric acid (0.5 M aqueous solution of citric acid at 353 K for 3 h) (removing of alumina debris). Finally, all the catalysts were calcined at 823 K for 3h. Considering the applied procedure for the treatment of catalysts, we used the following catalyst designations. Parent forms of ZSM5, Beta and Mordenite are marked as H-ZSM5(P), H-Beta(P), and H-Mordenite(P), respectively. The hierarchical zeolites after two-step modification (desilication process and further treatment with citric acid) are marked as follows: H-ZSM5(H), H-Beta(H), and H-Mordenite(H).

3. Characterization of catalysts

3.1. Textural properties (XRD, SEM, TEM, and sorption measurements)

The crystalline structure of the parent and modified zeolites was confirmed on the basis of X-ray diffraction patterns (XRD) recorded on a Bruker AXS D8 Advance diffractometer equipped in Cu Kα radiation. The relative crystallinity was calculated according to equation 1.[48]

$$\alpha = \alpha_o \times I/I_o \qquad \text{(Eq.1)}$$

where α_o is equal to 100, I and I_o are the areas of the reflexes characteristic of parent and modified zeolites, respectively. The I and I_o values indicate the sum of the areas of the most intense peaks at 2 Theta: 23.1-24.4° for ZSM5 zeolite, 22.5° for Beta zeolite, and 25.8-27.8° for Mordenite.

The morphology of the catalysts were examined using both scanning electron microscopy (SEM, Hitachi SU3500) and transmission electron microscopy (TEM, Hitachi HT7700) with an accelerating voltage of 100 kV.

N_2 adsorption-desorption at 77 K was performed in a Quantachrome Nova1000e analyzer on samples activated in vacuum at 573 K for 24 h. BET (Brunauer–Emmett–Teller) method was applied to calculate the total surface area, while the mesopores volume and the external surface area were evaluated by the t-plot method. The BJH pore size distributions were derived from the adsorption branch.

3.2. Elemental analysis

Si/Al ratio was evaluated by means of atomic absorption spectrometry with acetylene-nitrous oxide flame atomization (F-AAS) using the 3D double-beam Shimadzu AA7000 analytical technique (Shimadzu), equipped with an ASC-7000 autosampler (Shimadzu).

3.3. Acidity

The presence of hydroxyl groups, localized in different zeolite structures, was noticed using FT-IR spectra in the range of 3200-3800 cm^{-1}. The measurements were performed on a Bruker–Vector 22 spectrometer. All spectra have been normalized to the equal weight. Self-supporting wafers of the samples (20 mg/cm^2) were prepared, weighed and placed inside a bespoke quartz IR cell. Prior to the measurements, the samples were heated at 673 K under vacuum.

The number and strength of acid sites were estimated on the basis of TPD (thermal programmed desorption) of NH_3. In a typical experiment, about 40 mg of sample was heated in He stream with a heating rate of 10 K/min up to 723 K and kept at that temperature for 0.5 h, then cooled down to 393 K and afterwards saturated with ammonia for 0.5 h. The physically adsorbed NH_3 was removed by purging with helium flow at 393 K for 1 h. The TPD analysis was conducted in a range of 373-973 K with a heating rate of 10 K/min. The desorbed NH_3 was recorded by a TCD analyzer.

Hydrophobicity index was calculated according to the formula proposed by E.-P.Ng and Mintova[47a] and Giaya et al..[47b]

$$HI = \frac{V_t - V_{>423\,K}}{V_t} \qquad \text{(Eq.2)}$$

where V_t - total pore volume obtained from N_2 adsorption measurements and $V_{>423\,K}$ relates to volume of water measured at temperature higher than 423 K (in our measurements it was 673 K) and calculated using the bulk liquid density for adsorbed water. According to applied definition, material with HI = 1 is defined as highly hydrophobic, while this with HI = 0 shows hydrophilic nature.

4. Catalytic reaction of glycerol ketalization

The catalytic reaction of solketal synthesis was carried out under atmospheric pressure at the temperature of 323 K in a continuous down-flow reactor heated with an electric furnace (Fig. S3).The reactor was loaded with a given amount of catalyst (0.5 g) with a glass wool as a bed supporter. To avoid the clogging, the catalyst was mixed with an amorphous silica in the weight ratio equal to 1 : 1. Both catalyst as well as silica were fractioned to the same particle size (sieve fraction 0.3–0.5 mm). Catalysts were pre-activated at 623 K for 0.5 h in a helium flow before catalytic run. The feed was a mixture of 4.8 ml of glycerol and 14.4 ml of acetone (corresponding to the molar ratio equal to 3 : 1 of acetone : glycerol) dissolved in methanol (3.8 ml). In a typical run, the feed containing acetone, glycerol and the additional solvent (methanol) was pumped continuously into the reactor with flow rate equal to 6.4 cm^3/h and WHSV equal to 3.4 h^{-1} (WHSV defined as the mass flow of glycerol [kg/h])/(mass of catalyst [kg]). The experiments with WHSV in the range of 3.4-8.4 h^{-1} have also been performed. The reaction products were collected every 30 min. and analyzed by GC (VARIAN CP-3800) equipped with a FID detector and a VF-5ms capillary column using toluene as an internal standard. The glycerol conversion was defined as the amount of converted glycerol divided by the amount of glycerol before reaction and expressed in % according to equation 3.

$$Glycerol\ conv. = \frac{mol\ of\ glycerol\ converted}{initial\ mol\ of\ glycerol} \times 100 \qquad \text{(Eq. 3)}$$

The selectivity to solketal was calculated taking the molar concentration of solketal formed, divided by the amount of reacted glycerol, and expressed in % according to equation 4.

$$S\ solketal = \frac{mol\ of\ \ solketal\ formed}{mol\ of\ glycerol\ converted} \times 100 \qquad \text{(Eq. 4)}$$

In addition to the solketal (2,2-dimethyl-1,3-dioxolane-4-methanol) (Scheme 1, product 1a), small amount of undesired 6-membered ring isomer (2,2-dimethyl-1,3-dioxan-5-ol) (Scheme 1, product 1b) was also recorded. The selectivity to isomer, expressed in %, was calculated according to equation 5.

$$S\ isomer = \frac{mol\ of\ isomer\ formed}{mol\ of\ glycerol\ converted} \times 100 \qquad \text{(Eq. 5)}$$

Yield of solketal, expressed in %, was calculated according to equation 6.

$$Y\ solketal = \frac{S\ solketal \times Glycerol\ conv.}{100} \qquad \text{(Eq. 6)}$$

Keywords: Glycerol ketalization, solketal formation, hierarchical zeolites, a continuous flow system

[1] M. Ayoub, A. Z. Abdullah, *Renew. Sust. Energ. Rev.* ***2012****, 16,* 2671-2686.
[2] a) B. Katryniok, H. Kimura, E. Skrzyńska, J.-S. Girardom, P. Fongarland, M. Capron, R. Ducoulombier, N. Mimura, S. Paul, F. Dumeignil*, Green Chem.* ***2011****, 13,* 1960-1979; b) J.-C. M. Monbaliu, M. Winter, B. Chevalier, F. Schmidt, Y. Jiang, R. Hoogendoorn, M. A. Kousemaker, C.V. Stevens, *Bioresource Technol.* ***2011****,* 102, 9304-9307.
[3] a) V. Rossa, Y. da S. P. Pessanha, G.Ch. Díaz, L. D. T. Câmara, S. B. C. Pergher, D. A. G. Aranda, *Ind. Eng. Chem. Res.* ***2017****, 56,* 479-488; b) M. R. Nanda, Y. Zhang, Z. Yuan, W. Qin, H. S. Ghaziaskar , C. Xu, *Renew. Sust. Energ. Rev.* ***2016****,* 56, 1022-1031; c) G.S. Dmitriev, A.V. Terekhov, L.N. Zanaveskin, S.N. Khadzhiev, K.L. Zanaveskin, A.L. Maksimov, *Russ. J. Appl. Chem.* ***2016****, 89,* 1619-1624.
[4] C. J. A. Mota, C. X .A. da Silva, N. Rosenbach, Jr., J. Costa, F. da Silva, *Energ. Fuel.* ***2010****, 24,* 2733-2736.
[5] a) A.R. Trifoi,; P. Ş. Agachi, T. Pap, *Renew. Sust. Energ. Rev.* ***2016****, 62,* 804-814; b) L. P. Ozorio, R. Pianzolli, M. B. S. Mota, C. J. A. Mota, *J. Braz. Chem. Soc.* ***2012****, 23,* 931-937.
[6] a) C. X. A. da Silva, C. J. A. Mota, *Biomass. Bioenerg.* ***2011****, 35,* 3547-3551; b) M. R. Nanda, Z. Yuan, W. Qin, H. S. Ghaziaskar, M.-A. Poirier, C. C. Xu, *Fuel* ***2014****, 117,* 470-477; c) J. Deutsch, A. Martin, H. Lieske, *J. Catal.* ***2007****, 245,* 428-435.
[7] M. Ricciardi, L. Falivene, T. Tabanelli, A. Proto, R. Cucciniello, F. Cavani, *Catalysts* ***2018****, 8,* 391.
[8] a) P. Ferreira, I.M. Fonseca, A.M. Ramos, J. Vital, J.E. Castanheiro, *Appl. Catal. B: Environ.* ***2010****, 98,* 94-99; b) S. Sandesh, A. B. Halgeri, G. V. Shanbhag, *J. Mol. Catal. A: Chemical* ***2015****, 401,* 73-80.
[9] G. Vincente, J. A. Melero, G. Morales, M. Paniagua, E. Martin, *Green Chem.* ***2010***, 12, 899-907.
[10] Li Li, Tamás I. Korányi, Bert F. Sels and Paolo P. Pescarmona, *Green Chem*., ***2012***, 14, 1611-1619.
[11] S. R. Churipard, P. Manjunathan, P. Chandra, G. V. Shanbhag, R. Ravishankar, P. V. C. Rao, G. S. Ganesh, A. B. Halgeri S. P. Maradur. *New J. Chem.,* ***2017***, 41, 5745-5751.
[12] a) M. R. Nanda, Z. Yuan, W. Qin, H. S. Ghaziaskar, M.-A. Poirier, C. C. Xu, *Appl. Energ.* ***2014****, 123,* 75-81; b) M. R. Nanda, Z. Yuan, W. Qin, H. S. Ghaziaskar, M.-A. Poirier, C.C. Xu, *Fuel* ***2014****, 128,* 113-119.
[13] M. Shirani, H. S. Ghaziaskar, C. Xu, *Fuel Process. Technol.* ***2014****, 124,* 206-211.
[14] P. A. Oliveira, R. O. M. A. Souza**,** C, J. A. Mota, *J. Braz. Chem. Soc.* ***2016****, 27,* 1832-1837.
[15] B. Yilmaz; U. Müller, Catalytic Applications of Zeolites in Chemical Industry, *Top. Catal.* ***2009****, 52,* 888-895.
[16] a) P. Manjunathan, S. P. Maradur, A. B. Halgeri, G. V. Shanbhag, J. *Mol. Catal. A: Chem.* ***2015****, 396,* 47-54; b) C. X. A. da Silva, V. L. C. Gonçalves, C. J. A. Mota*, Green Chem.,* ***2009****, 11,* 38-41.
[17] a) X. Gao, X. Zou, F. Zhang, S. Zhang, H. Ma, N. Zhao, G. Zhu, *Chem. Commun., 2013, 49* 8839-8841; b) M. P. Bernal, E. Piera, J. Coronas, M. Menéndez, J. Santamaria, *Catal. Today* ***2000****, 56,* 221-227.
[18] B. Mallesham, B. G. Rao, B. M. Reddy, *C. R. Chimie* ***2016****, 19,* 1194-1202.
[19] a) J. C. Groen, T. Sano, J. A. Moulijn, J. Pérez-Ramírez, *J. Catal.* ***2007****, 251,* 21-27; b) J. C. Groen, J. A. Moulijn, J. Pérez-Ramírez, *Micropor. Mesopor. Mat.* ***2005****, 87,* 153-161.
[20] Y. Gao, B. Zheng, G. Wu, F. Ma, C. Liu, *RSC Adv.* ***2016****, 6,* 83581-83588.
[21] C. Gonzalez-Arellano, A. Grau-Atienza, E. Serrano, A. A. Romero, J. Garcia-Martinez, R. Luque, *J. Mol. Catal. A: Chem.* ***2015****, 406,* 40-45.
[22] H. Zhang, Z. Hu, L. Huang, H. Zhang, K. Song, L. Wang, Z. Shi, J. Ma, Y. Zhuang, W. Shen, Y. Zhang, H. Xu, Y. Tang, *ACS Catalysis* ***2015****, 5,* 2548-2558.
[23] A. Shahid, S. Lopez-Orozco, V. Reddy Marthala, M. Hartmann, W. Schwieger, *Micropor. Mesopor. Mat.* ***2017****, 237,* 151-159.
[24] a) X.-F. Zhang, K. Zhang, X. Zhang, Y. Feng, J. Yao, *Micropor. Mesopor. Mat.* ***2018****, 272,* 202-208; b) Y. Wang, Y. Sun, C. Lancelot, C. Lamonier, J.-C. Morin, B. Revel, L. Delevoye, A. Rives, *Micropor. Mesopor. Mat.* ***2015****, 206,*

42-51; c) L. Zhao, J. Gao, C. Xu, B. Shen, *Fuel Process. Technol.* ***2011****, 92,* 414-420.
[25] S. Ban, A. N. C. van Laak, J. Landers, A. V. Neimark, P. E. de Jongh, K. P. de Jong, T. J. H. Vlugt, *J. Phys. Chem. C* ***2010****, 114,* 2056-2065.
[26] a) G. Liu, M. Jia, Z. Zhou, L. Wang, W. Zhang, D. Jiang, *J. Colloid and Interf. Sci.* ***2006****, 302,* 278-286; b) J. M. Campelo, D. Luna, R. Luque, J. M. Marinas, A. A. Romero, J. J. Calvino, M. P. Rodríguez-Luque, *J. Catal.* ***2005****, 230,* 327-338.
[27] J. C. Groen, L. A. A. Peffer, J. Pérez-Ramírez, *Micropor. Mesopor. Mat.* ***2003****, 60,* 1-17.
[28] K. Smith, G. A. El-Hiti, *Green Chem.* ***2011****, 13,* 1579-1608.
[29] V. Paixao, R. Monteiro, M. Andrade, A. Fernandes, J. Rocha, A. P. Carvalho, A. Martins, *Appl. Catal. A: General* ***2011****, 402,* 59-68.
[30] M. Ogura, S. Shinomiya, J. Tateno, Y. Nara, M. Nomura, E. Kikuchi, M. Matsukata, *Appl. Catal. A: General* ***2001****, 219,* 33-43.
[31] H. Tao, H. Yang, X. Liu, J. Ren, Y. Wang, G. Lu, *Chem. Eng. J.* ***2013****, 225,* 686-694.
[32] X. Li, R. Prins, J. A. van Bokhoven, *J. Catal.* ***2009****, 262,* 257-265.
[33] S. Stefanidis, K. Kalogiannis, E. F. Iliopoulou, A. A. Lappas, J. M. Triguero, M. T. Navarro, A. Chica, F. Rey, *Green Chem.* ***2013****, 15,* 1647-1658.
[34] D. Verboekend, S. Mitchell, M.Milina, J.C. Groen, J .Pérez-Ramírez, *J. Phys. Chem. C* ***2011****, 115,* 14193-14203.
[35] K. Sadowska, K. Góra-Marek, M. Drozdek, P. Kuśtrowski, J. Datka, J. M. Triguero, F. Rey, *Micropor. Mesopor. Mater.* ***2013****, 168,* 195-205.
[36] B. Gil, Ł. Mokrzycki, B. Sulikowski, Z. Olejniczak, S. Walas. *Catal. Today* ***2010****, 152,* 24-32.
[37] K. Góra-Marek,.K. Tarach, J. Tekla, Z. Olejniczak, P. Kuśtrowski, L. Liu, J. Martinez-Triguero, F. Rey, *J. Phys. Chem. C* ***2014****, 118,* 28043-28054.
[38] Y.-Q. Song, Y.-L. Feng, F. Liu, C.-L. Kang, X.-L. Zhou, L.-Y. Xu, G.-X. Yu, *J. Mol. Catal. A: Chem.* ***2009****, 310,*130-137.
[39] N. J. Venkatesha, Y. S. Bhat, B. S. Jai Prakash, *RSC Adv.****2016****, 6,* 18824-18833.
[40] J. Kowalska-Kus, A. Held, K. Nowinska, *Reac. Kinet. Mech. Cat.* ***2016****, 117,* 341-352.
[41] K. Barbera, F. Bonino, S. Bordiga, T. V. W. Janssens, P. Beato*, J. Catal.* ***2011***, 280, 196-205.
[42] S.-T. Tsai, P.-Y. Chao, P.-H. Chao, K.-J. Du, M.-J. Fang, S.-B. Liu, T.-C. Tsai, *Catal. Today* ***2016****, 259,* 423-429.
[43] B. Wang, C. W. Lee, T.-X. Cai, S.-E. Park, *Catal. Lett.* ***2001****, 76,* 99-103.
[44] S.-T. Tsai, C.-H. Chen, T.-C. Tsai, *Green Chem.* ***2009****, 11,* 1349-1356.
[45] M Thommes, S. Mitchell, J. Pérez-Ramírez, *J. Phys. Chem. C* ***2012***, 116, 18816-18823.
[46] A. H. Yonli, I. Gener, S. Mignard, *Micropor. Mesopor. Mat.* ***2010****,* 132, 37-42.
[47] a) E.-P.Ng, S. Mitova, *Micropor. Mesopor. Mat.* ***2008****,* 114, 1-26; b) A. Giaya, R. W. Thompson, R. Denkewicz Jr., *Micropor. Mesopor. Mat.* ***2000***, 40, 205-218.
[48] M. D. González, Y.Cesteros, P.Salagre, *Micropor. Mesopor. Mater.* ***2011,*** *144,* 162-170.

Entry for the Table of Contents (Please choose one layout)

Layout 1:

FULL PAPER

Hierarchical H-Beta(H) and H-ZSM5(H) zeolites demonstrates their superior performance in the reaction of glycerol with acetone ketalization carried out in a flow-system at low temperature and under atmospheric pressure. The larger pore size, created as a desilication effect in hierarchical zeolites, allows to avoid diffusion restriction of reagents and facilitates contact of the reactants with the active centers, resulting in a very high activity in the studied process.

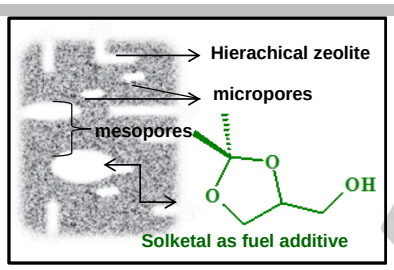

*Agnieszka Held, Krystyna Nowińska, Jolanta Kowalska-Kuś**

Page No. – Page No.

Solketal formation in a continuous flow process over hierarchical zeolites

Layout 2:

FULL PAPER

((Insert TOC Graphic here; max. width: 11.5 cm; max. height: 2.5 cm))

*Author(s), Corresponding Author(s)**

Page No. – Page No.

Title

Text for Table of Contents